

## Distribution of attraction basins in a family of simple glasses

This article has been downloaded from IOPscience. Please scroll down to see the full text article.

2000 J. Phys.: Condens. Matter 12 6641

(<http://iopscience.iop.org/0953-8984/12/29/335>)

View [the table of contents for this issue](#), or go to the [journal homepage](#) for more

Download details:

IP Address: 171.66.16.221

The article was downloaded on 16/05/2010 at 05:24

Please note that [terms and conditions apply](#).

## Distribution of attraction basins in a family of simple glasses

P Chandra<sup>†</sup> and L B Ioffe<sup>‡§</sup>

<sup>†</sup> NEC Research Institute, 4 Independence Way, Princeton, NJ 08540, USA

<sup>‡</sup> Landau Institute for Theoretical Physics, Moscow, Russia

<sup>§</sup> Department of Physics, Rutgers University, Piscataway, NJ 08855, USA

Received 2 May 2000

**Abstract.** We study the distribution of attraction basins as a function of energy in simple glasses. We find that it is always broad. Furthermore, we identify two types of glass, both with an exponentially large number of metastable states. In one type the largest attraction basin is exponentially small, whereas in the other it is polynomially small in the system size  $N$ . If there exists a tuning parameter that connects one regime with another, then these two phases are separated by a critical point. We discuss implications for optimization problems.

(Some figures in this article appear in colour in the electronic version; see [www.iop.org](http://www.iop.org))

### 1. Introduction

A complex system is one whose number of metastable configurations,  $N_s$ , scales exponentially with the number of its elements,  $N$ . Naively one expects that an exponential number of searches is required to find the optimal state. In general the identification of the ground state in a complex system can be mapped onto a hard combinatorial optimization problem [1]. However, there exist examples in nature, e.g. proteins [2–5], of complex systems that find their ground states on timescales significantly faster than  $\tau \sim N_s$ . A possible explanation for this phenomenon is that the associated total phase volume is not equally divided among the metastable states. More specifically, if a significant fraction of the total phase volume belongs to the attraction basin of the optimal state, then a fast process leading to this ‘greedy’ configuration becomes feasible to implement. A less stringent possibility is that the optimal state can be located relatively quickly if it is connected by a continuous path in the space of parameters to a state with a large basin of attraction. This is the underlying approach in simulated annealing, an optimization algorithm that is very effective for problems where the ground state evolves continuously from the paramagnetic configuration as a function of decreasing temperature [6]. However simulated annealing cannot be applied to systems where all the metastable states appear at the same temperature [7, 8]. In this case an open question is whether one can identify a parameter that connects the state continuously to one with a large basin of attraction. We have addressed this issue in a family of simple glasses characterized by a parameter  $x$ . In particular we find that this parameter can be increased continuously such that there exists a small subset of metastable states which attract the system with significant probability  $\mathcal{P}$  such that

$$\frac{1}{N} \ln \frac{1}{\mathcal{P}} \ll 1$$

in contrast to the generic situation

$$\frac{1}{N} \ln \frac{1}{\mathcal{P}} \sim 1$$

in complex systems.

Here we study the basins of attraction in a family of  $p$ -spin spherical models [9] characterized by the Hamiltonian

$$H = \sqrt{x} \sum_{i_1 i_2} J_{i_1 i_2} s_{i_1} s_{i_2} + \sqrt{1-x} \sum_{i_1 i_2 i_3} J_{i_1 i_2 i_3} s_{i_1} s_{i_2} s_{i_3} \quad (1)$$

where the constraint  $\sum_{i=1}^N s_i^2 = 1$  is satisfied by the  $N$  spins that are represented by real variables  $s_i$ .  $J_{i_1 i_2}$  and  $J_{i_1 i_2 i_3}$  are two- and three-spin infinite-range couplings respectively; furthermore they are completely random in sign and in amplitude, and are uncorrelated. In this family of glasses, we find that the configurational entropy,  $\mathcal{S}_c \equiv \ln N_s$ , remains extensive ( $\mathcal{S}_c \propto N$ ) for  $0 \leq x < 1$  whereas  $\mathcal{S}_c = 0$  for precisely  $x = 1$ . This limit corresponds to the  $p = 2$  disordered spherical model which has only one locally stable solution [10] and therefore an associated basin of attraction that is large. The other extreme parameter limit of (1),  $x = 0$ , corresponds to the three-spin spherical model with an extensive number of metastable states [11, 12] whose attraction volumes are each an exponentially small fraction of the full phase space [13]. As an aside, we note that here we will use the normalizations

$$\langle J_{i_1 i_2}^2 \rangle = \frac{1}{8N} \quad (2)$$

$$\langle J_{i_1 i_2 i_3}^2 \rangle = \frac{1}{36N^2} \quad (3)$$

where the angular brackets refer to an average over disorder; these expressions, (2) and (3), are slightly different than those commonly found in the literature but are convenient for this family of mixed models.

The  $p$ -spin random spherical models ( $p > 2$ ) are believed to be the simplest models that possess the essential properties of a generic complex system [14]. Aside from having an extensive complexity ( $\mathcal{S}_c \propto N$ ), they also exhibit history dependence and aging characteristic of experimental glasses [15]. The simplicity of these models arises from the long-range nature of the interactions, a feature that makes them accessible to direct analytic treatment; second, all metastable states appear at some temperature and do not further bifurcate; third, the most probable overlap between two states is zero in the thermodynamic limit [9, 16], and furthermore all overlaps are bounded from below [17], a feature which simplifies the dynamical equations for  $N_s \rightarrow \infty$ . Naturally the evolution of a particular system with specific couplings must be studied numerically. However, the physical properties of the system averaged over all possible realizations of couplings can be studied analytically using a set of integral–differential equations [18, 19]. The latter describe the properties of typical metastable states where stochastic processes will take the averaged system. Here we show that the solution of these equations implies that for  $x = 0$  ( $p = 3$  spherical model) the distribution of attraction basins as a function of energy is broad, though the attraction volume associated with the ground state is still an exponentially small part of the full phase space [13]. This regime persists up to finite  $x_c \sim \frac{1}{2}$ . However, we find that as we continuously tune  $x$  to  $x > x_c$  the complexity remains extensive ( $\mathcal{S}_c \propto N$ ) for  $x_c < x < 1$  but the ground state acquires a large basin of attraction that far exceeds the average and is a significant fraction of the total phase volume.

We extract the distribution of attraction basins from the dynamical equations of the mixed model (1) as a function of  $x$ . More specifically, we relate the size of an attraction basin associated with a physical state to the critical overlap,  $q^*$ , between this state and a partially randomized one that still evolves back to it. In particular, the limit  $q^* \rightarrow 0$  corresponds to a basin of attraction that occupies a significant portion of the available phase volume. The critical overlap  $q^*$  is found from the solutions of the dynamical equations of (1).

The outline of this paper is as follows. In section 2 we discuss the general approach taken here, in particular the determination of the critical overlap as a function of energy,  $q^*(E)$ . In section 3 we apply this approach to the pure  $p = 3$  random spherical model and study the attraction basins as a function of energy. Next we turn to the mixed model (1) and determine the distribution of attraction basins for different values of  $x$ . We find a parameter regime,  $1 > x > x_c$ , where the mixed model has a typical state with large trapping probability ( $(1/N) \ln(1/\mathcal{P}) \ll 1$ ); furthermore in this regime the mixed model has marginally stable states. In section 4 we summarize our results in a discussion, noting that this conclusion is based on a study of dynamical equations that appear in a broad class of glassy models [20]; in particular they also describe glassy systems without quenched disorder [21–24]. These equations have also been proposed on phenomenological grounds for the description of freezing in structural glasses; they are the so-called mode-coupling equations [25]. Thus we expect our result to be more general than the specific mixed model defined above.

## 2. The approach

The key step in our approach is to extract the probability,  $\mathcal{P}$ , with which the typical state attracts the system from the dynamical equations of the  $p$ -spin model. This probability,  $\mathcal{P}$ , is equal to the ratio of the attraction basin of the physical state,  $W_B$ , and the full volume of phase space,  $W_{PH}$ , so  $\mathcal{P} = W_B/W_{PH}$ . We take the typical state as a reference point and parametrize arbitrary points in phase space by their respective angles to this configuration. In this framework,

$$W_{PH} = \mathcal{N}^{N-2} \int_0^\pi d\theta \sin^{N-2} \theta \quad (4)$$

where  $\mathcal{N}^{N-2}$  is the volume of the  $(n - 2)$ -dimensional unit sphere. Similarly the volume of the attraction basin of the reference state is

$$W_B = \mathcal{N}^{N-2} \int_0^\pi d\theta P(\theta) \sin^{N-2} \theta \quad (5)$$

where  $P(\theta)$  is the probability that the state at angle  $\theta$  belongs to the basin of attraction associated with the reference configuration.

We note that for  $N \gg 1$  the main contribution to  $W_{PH}$  in (5) arises from  $\sin \theta \equiv 1$ , whereas that of  $W_B$  comes from the largest possible  $\sin \theta$  such that  $P(\theta)$  is finite. Therefore the behaviour of  $P(\theta)$  for  $\theta \sim \pi/2$  is crucial for this discussion. It is therefore convenient to rewrite the expressions for  $W_{PH}$  and  $W_B$  using the parametrization  $q = \cos \theta$  where  $q$  is the overlap between the typical state and that at angle  $\theta$ . In this notation, assuming that  $N \gg 1$ , we find that

$$W_{PH} = \mathcal{N}^{N-2} \int_0^\infty dq e^{-(N/2)q^2} \quad (6)$$

and

$$W_B = \mathcal{N}^{N-2} \int_0^\infty dq P(q) e^{-(N/2)q^2} \quad (7)$$

where we note that the main contribution to  $W_{PH}$ , displayed in (6), arises from small  $q \sim 1/\sqrt{N}$ . There are two possible scenarios:

- (i)  $P(q) \equiv 0$  for  $q < q^*$  (where  $q^* > 1/\sqrt{N}$ ). We note that this threshold coincides with the previous definition of  $q^*$ , the critical overlap beyond which a partially randomized state evolves away from the reference state. In this case

$$\mathcal{P} = \frac{W_B}{W_{PH}} \propto e^{-(N/2)(q^*)^2} \quad (8)$$

and

$$\frac{1}{N} \ln \frac{1}{\mathcal{P}} \sim 1. \tag{9}$$

(ii)  $P(q) = f(q)$ , so there is no threshold (i.e.  $q^* \rightarrow 0$ ).

Then the probability that the reference state attracts the system is *not* exponentially small and

$$\frac{1}{N} \ln \frac{1}{\mathcal{P}} \ll 1. \tag{10}$$

Therefore the size of the attraction basin associated with the typical state is determined by the value of the critical overlap  $q^* \equiv \cos \theta^*$ . We expect  $q^*$  to have a distribution of finite width; in this case states with the smallest value of  $q^*$  will have exponentially larger attraction basins than the others. Furthermore, if  $q^* \rightarrow 0$  then these states will have basins of attraction that are a significant fraction of the full phase volume.

We now discuss how to extract  $P(q)$  and  $q^*$  from the dynamical equations of the family of  $p$ -spin spherical models. These equations determine the time evolution of averaged correlation ( $D_{tt'} = \langle s(t)s(t') \rangle$ ) and response ( $G_{tt'} = \langle \partial s(t) / \partial h(t') \rangle$ ) functions for arbitrary sample history. In order to find  $P(q)$ , we consider the evolution of a state where at time  $t_0$  a fraction  $1 - q$  of the total spins is randomized so that at time  $t_0 + \epsilon$  the system is in a random state corresponding to overlap  $q$  with the state at  $t_0$ . In terms of  $D_{tt'}$  and  $G_{tt'}$  this randomization translates into the boundary conditions

$$D_{t_0+\epsilon, t'} = (1 - q)D_{t_0 t'} \tag{11}$$

$$G_{t_0+\epsilon, t'} = (1 - q)G_{t_0 t'} \tag{12}$$

where  $t_0 > t'$ . The solution of the dynamical equations yields  $Q(q) \equiv \lim_{t \rightarrow \infty} D_{t t_0 - \epsilon}(q)$ , the average overlap between a typical state and that which has evolved from it in the manner described above. This quantity can be interpreted in a simple way if all metastable states are orthogonal; in this case  $Q(q)$  is equal to  $P(q)$ , the probability that the system evolves back to its original configuration after a fraction  $(1 - q)$  of the spins have been randomized. This is indeed the situation for the family of spherical spin models that we study here where there is only one-step replica-symmetry breaking as in the pure  $p = 3$  spherical model [9]; details of the replica solution for the mixed models are presented in appendix A.

We note that  $Q(q)$  depends implicitly on the properties of the typical state at time  $t_0$ . The dynamical equations with random initial conditions yield  $Q(q)$  averaged over all typical states. This average is dominated by the states for which the combined basin of attraction is maximal; for instance if states are characterized by their energy, this quantity  $N(E)W_B(E)$  is usually largest for states with the highest energy which are still stable, namely states that are marginally stable. In order to probe states with different energies, one needs to introduce different initial conditions via source terms in the dynamical equations [26–29]. The solution of these modified equations yields  $Q(q, E)$ , the overlap averaged over typical states of fixed energy  $E$ .

The dynamical equations for the family of spherical models with Hamiltonian (1) at  $t < t_0$  and at  $t > t_0$  have the form

$$\dot{s}_i = -\Gamma \frac{\partial H(x)}{\partial s_i} + \eta_i(t) \quad \langle \eta_i(t)\eta_j(t') \rangle = 2T\Gamma \delta_{ij} \delta(t - t') \tag{13}$$

which reduces to the set of equations

$$(a_{t_1} + \partial_{t_1})D_{t_1 t_2} - 2G_{t_1 t_2} - \frac{\beta^2}{2} \int \Pi_{t_1 t} G_{t t_2} dt - \frac{\beta^2}{2} \int \Sigma_{t_1 t} D_{t t_2} dt = \mathcal{S}_D \tag{14}$$

and

$$(a_{t_1} + \partial_{t_1})G_{t_1 t_2} - \frac{\beta^2}{2} \int \Sigma_{t_1 t} D_{t t_2} dt = \delta(t_1 - t_2) \tag{15}$$

where  $\beta$  is the inverse temperature,  $\Sigma$  and  $\Pi$  are self-energy terms,  $a_t$  is determined implicitly by the condition  $D_{tt} = G_{tt} = 1$ , and  $S_D$  is a source term that fixes the initial energy. For this mixed model with  $N \gg 1$ , we have

$$\Sigma_{t_1 t_2} = 2(1 - x)(GD)_{t_1 t_2} + xG_{t_1 t_2} \tag{16}$$

$$\Pi_{t_1 t_2} = (1 - x)D_{t_1 t_2}^2 + xD_{t_1 t_2} \tag{17}$$

and

$$S_D = \frac{6\beta E_0}{2 + x} (D_{t_1 0}^2 D_{t_2 0} (1 - x) + xD_{t_1 0} D_{t_2 0}) \tag{18}$$

where  $E_0$  is the energy of the initial configuration at  $t = 0$ . In the two self-energies, equations (16) and (17), we recover known results for the  $p = 2$  and  $p = 3$  spherical models for  $x = 1$  and  $x = 0$  respectively [18,19]. The source term, equation (18), is derived by introducing a term  $\delta(H(t = 0) - E_0)$  into the functional integral for the stochastic dynamics, representing it as an additional integral over a Lagrangian multiplier where the latter is determined by the initial energy  $E_0$ . In order to obtain  $P(x, q, E)$ , we solve this system of equations varying these three parameters.

### 3. Results

In figure 1 we display the spin–spin correlation function,  $D_{t t'}$ , of the  $x = 0$  ( $p = 3$ ) spherical model after a fast quench (i.e. with random initial conditions) as a reference starting point for our subsequent discussion. Apart from a narrow range  $t' \approx t$ , this correlation function obeys a scaling [19] form  $D_{t t'} \sim (t'/t)^\gamma$ .

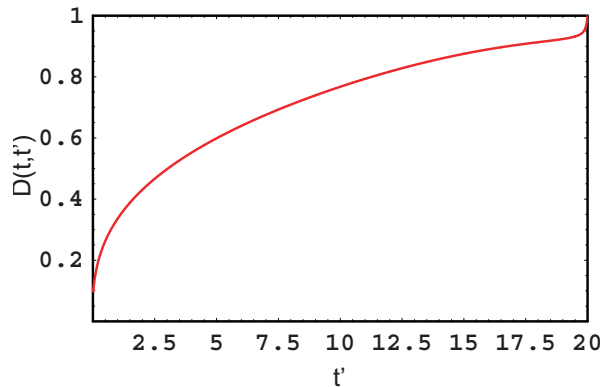


**Figure 1.** The spin–spin correlation function after a fast quench at  $T = \frac{1}{4}T_c$  for the  $p = 3$  spherical model. Note the fast relaxation at very short  $t - t' \ll 1$ .

In figure 2 we show the correlation function for the solution when the system was partially randomized at  $t_0 = t/2$  as described in (11) and (12). As an aside, we note that here and in what follows we present results for  $t/t_0 = 2$ ; we have checked that they are weakly dependent on this ratio. As expected, increased randomization leads to a decreasing overlap between the state at  $t_0$  and at  $t = 2t_0$ . We also note that  $D_{t_1 t_2}$  shows power-law aging behaviour,  $D_{t_1 t_2} \approx (t_1/t_2)$ ,

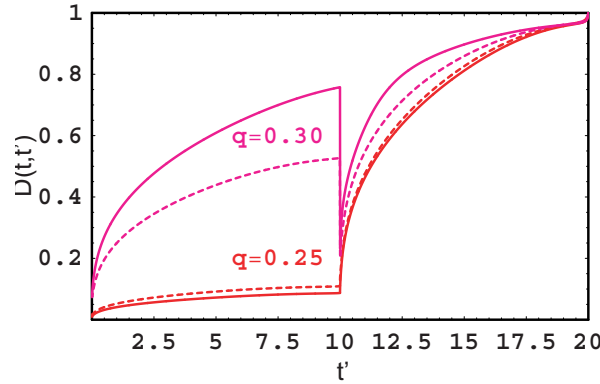


**Figure 2.** The spin–spin correlation function for the  $p = 3$  spherical model after a fast quench to  $T = \frac{1}{8}T_c$  followed by a randomization to  $t_0 = \frac{1}{2}t$  with different fractions,  $(1 - q)$ , of the total number of spins affected. Dashed lines refer to the results for the total time  $t = 10$  rescaled to those for  $t = 20$ . These data indicate that  $0.25 < q^* < 0.30$  since an increase in the total time  $t$ , keeping the ratio  $t_0/t$  fixed, leads to evolution in different directions of  $Q(q) \equiv \lim_{t \rightarrow \infty} D_{t_0-\epsilon}(q)$ .

for  $t_1, t_2 < t_0$ ; for  $t_1, t_2 > t_0$  the relaxation starts again and  $D_{t_1 t_2} = d((t_2 - t_0)/(t_1 - t_0))$ . These curves were determined numerically for finite  $t_0$ ; as  $t_0 \rightarrow \infty$  we expect the limiting value of these overlaps to tend either to the self-overlap,  $Q_0$ , or to zero slowly. For example, a factor-of-two increase in the overall time changes  $D_{tt'}$  a little bit as displayed in figure 2 by the dashed and full curves. Therefore a systematic finite-time analysis is necessary to determine the value of  $q^*$ . The dashed and full curves presented in figure 2 indicate that  $q^*$  lies between  $q_1$  and  $q_2$  because the plot for  $q_1$  decreases with increasing  $t_0$  whereas the opposite is true for  $q_2$ . We note that the slow decrease in  $Q(q_1)$  with overall time can be understood as a finite-time effect; more specifically,  $Q(q_1)$  follows the same time evaluation as  $D_{t_0}$  for the reference dynamics without randomization (see figure 1) such that

$$\frac{\ln D_{t_0+\epsilon, t_0}}{\ln t} = \frac{\ln D_{t, 0}}{\ln t} = -\frac{1}{4}. \quad (19)$$

In order to obtain  $q^*$  more precisely, we consider the derivative  $dQ(q, t)/d \ln t$  at finite  $t$  with  $t_0$  always fixed at  $t_0 = \frac{1}{2}t$ . We determine  $q^*$  from the equation  $dQ(q, t)/d \ln t = 0$  where we check that the value of  $q^*$  obtained in this fashion is not dependent on the overall measuring time. We note that the result, namely that  $q^*(E = 0)$  is finite for  $x = 0$  ( $p = 3$  spherical model), is consistent with the conclusions of an earlier study of this model [13]. Furthermore we have checked that this result is not sensitive to our specific choice of the ratio  $t_0/t$ .

Until now, we have considered solutions to the dynamical equations, (14) and (15), with random initial conditions; as we have discussed earlier, these probe high-energy states that are marginally stable, a feature that is responsible for their power-law evolution. We now turn to lower-energy states as shown in figure 3. In order to access them we must fix our initial energy to be  $E_0 < E_C$ . In figure 4 we display typical spin–spin correlation functions in this energy regime. The two upper curves indicate clearly that for sufficiently large  $q$  the system recovers its state at  $t_0$ . For smaller  $q$  the state at  $t_0 + \epsilon$  evolves away from its reference state (see figure 4) in a manner similar to that for  $D_{tt'}$  with completely random initial conditions (see figure 1). Despite this qualitatively different behaviour for large and small  $q$ ,  $q^*$  must be determined by the same finite-time scaling as was discussed earlier. Such an analysis indicates that  $q^*(x = 0, E)$  remains finite for all energies. Therefore the basins of attraction in the  $p = 3$  spherical model increase with decreasing energy, but always remain exponentially

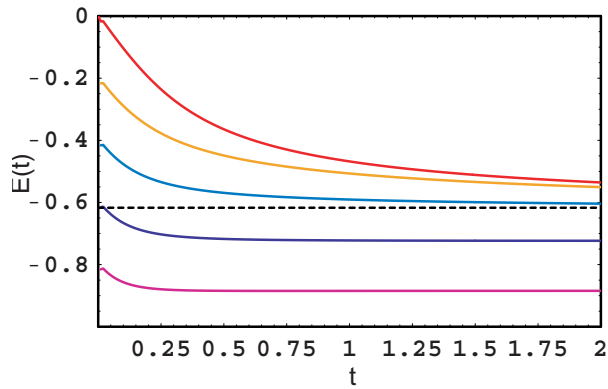


**Figure 3.** The energy dependence of the dynamical solutions for the  $p = 3$  spherical model with different initial energies. Note that for all initial energies  $E(0) > -0.4$  the energy approaches its asymptotic value ( $E(\infty) = -0.61$ , indicated by the dashed line) with power-law decay; by contrast for  $E_0 < -0.4$  the energy behaviour is exponential and  $E(\infty)$  depends on  $E(0)$ . Note also that the exponential relaxation time  $\tau_0 \sim 0.1$  in our units.

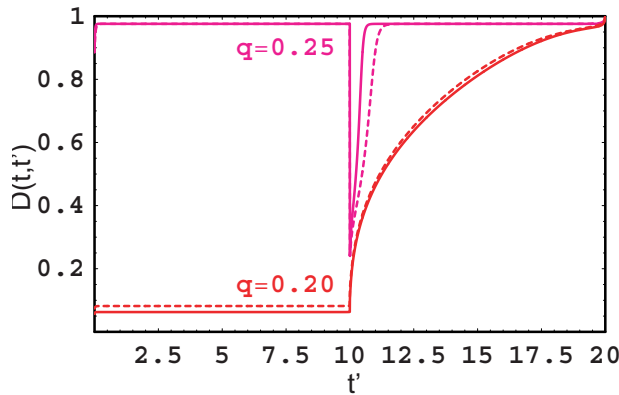


**Figure 4.** The spin-spin correlation function for the  $p = 3$  model with  $E(0) = -0.6$  (corresponding to exponential relaxation) with  $T = \frac{1}{8}T_c$  with randomization at  $t_0 = \frac{1}{2}t$ . Note that for  $q = 0.25$  the randomization is followed by very fast relaxation back to the initial state. By contrast, a slightly larger randomization  $q = 0.20$  (corresponding to the randomization of  $(1 - q) = 0.80$  of the total spins) leads to a completely different states similar to that found after a fast quench. We comment that  $t = 20$  corresponds to  $t/\tau_0 \approx 200$ .

small compared with the full phase volume [13].

In weakly frustrated systems where the number of metastable states is subexponential, some basins of attraction must be large. An example of such a system is the  $p = 2$  spherical model [10]. An interesting question is that of whether it is possible to have some large basins of attraction but an exponential total number of states. We expect an exponential number of states in a mixed  $p = 2$  and  $p = 3$  spherical model, and therefore study a family of such systems to see whether they ever acquire typical states with large basins of attraction.

We have checked that there is one-step replica-symmetry breaking for  $0 \leq x \leq 1$ , and details are presented in appendix B. As a result, we know that all metastable states appear at  $T = T_c$  and that there is no further subdivision of states at lower temperatures. We can therefore perform an enumeration of these configurations at  $T = 0$ . We have verified by direct



computation that the logarithm of the number of states for this mixed model is

$$S_C \equiv \ln \mathcal{N}(x) = \frac{N}{2} \left( 2 + \ln(2-x) - \frac{24(2-x)}{(x+2)(3-x)^2} \right) \quad (20)$$

which is zero only at  $x = 1$  ( $p = 2$ ) where  $x$  is a mixing parameter as defined in the Hamiltonian (1). Details of the calculation that yields (20) are given in appendix B.

We repeated the numerical analysis outlined above for values of  $x$  such that  $0 < x < 1$ . Our results for  $q^*$  are summarized in figure 5. As shown there, for  $x = 0.3$  all basins of attraction remain exponentially smaller than the full phase volume. However, for  $x = 0.6$ , the critical overlap  $q^*(E)$  is zero at  $E_0$  indicating that states of energy  $E_0$  have basins of attraction that occupy a significant fraction of the full phase volume.

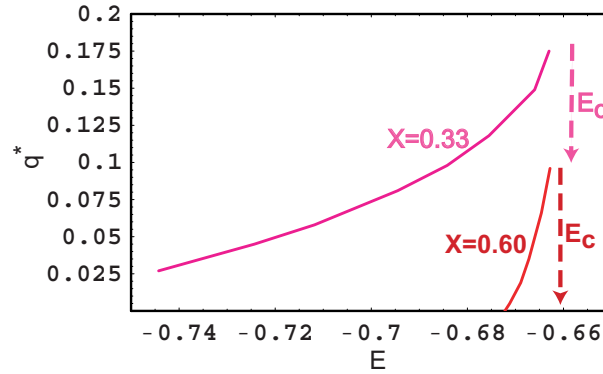


**Figure 5.** The critical overlap,  $q^*$ , as a function of initial energy,  $E = E(0)$ , for  $x = 0.33$  ( $x < x_c$ ) and  $x = 0.60$  ( $x > x_c$ ). We note that in the latter case  $q^*(E)$  crosses the  $x$ -axis, indicating the appearance of a state with a large attraction volume.

Now we discuss possible weak points in this argument. We have assumed the exact orthogonality of the metastable states which is only true to order  $1/\sqrt{N}$ . This might lead to  $q^* \sim 1/\sqrt{N}$  instead of  $q^* = 0$  for the states with large attraction basins. This correction would result in  $\mathcal{P} \sim N^{-\alpha}$  with  $\alpha$  of order unity. Another weak point in the argument might be the effect of finite-size corrections to the equations (11)–(17) which were originally derived in the thermodynamic limit. For the  $p = 3$  spherical model we have derived the subleading terms in  $1/N$  which modify the expressions for the self-energies  $\Sigma$  and  $\Pi$ , included them in equations (14) and (15), and have checked that their effects are perturbative. Furthermore, because the self-energy scales as  $D^3$ , higher-order terms in  $1/N$ , e.g. terms  $O(1/N^3)$ , cannot change the solution of equations (14) and (15) for  $D > 1/N^{2/3}$  and thus cannot lead to  $q^* > 1/\sqrt{N}$ . Therefore in the mixed  $p$ -spin models we expect higher-order terms in  $1/N$  to only lead to power-law corrections in  $\mathcal{P}$ , and thus to not qualitatively affect our results for  $(1/N) \ln(1/\mathcal{P})$ . Naturally there are also non-perturbative effects, but their contributions would not change the qualitative nature of our results.

#### 4. Discussion

We have studied the attraction volume of a typical state of energy  $E$  in a family of disordered spherical spin models which interpolate between  $p = 3$  (extensive configurational entropy) and  $p = 2$  (one stable solution) as a function of a tuning parameter  $x$ . For  $0 \leq x < 1$  the total number of metastable states is exponential in  $N$ . We find that for small  $x$  (i.e. close to the

$p = 3$  model) the largest attraction basin is an exponentially small fraction of the full phase volume; this is true despite the fact that it is a strongly varying function of energy. We also find that for  $x > x_c \sim 0.5$  (more precisely, we could only bracket it by  $0.3 < x_c < 0.6$ ) the largest attraction basin constitutes a significant part of the full phase volume, although the total number of states remains exponential. We did not find any thermodynamic signatures at  $x = x_c$ , and thus believe that *only* the dynamical behaviour of these glasses changes qualitatively at this critical point. We note that the singularity is approached as a function of decreasing  $x$  with increasing randomness in the models. Furthermore, the critical point described here separating polynomially and exponentially small reduced attraction volumes ( $\mathcal{P} = W_B/W_{PH}$ ) as a function of  $x$  bears a striking resemblance to that studied recently in  $K$ -satisfiability problems [30].

An important open question is the physical origin of the state with large attraction volume that appears for  $1 > x \geq x_c$ . At  $x = 1$  its presence is not surprising because there exists only one stable solution. It seems plausible that this state evolves continuously with decreasing  $x$  and retains its large attraction volume until  $x = x_c$ ; this has been confirmed by complementary numerical studies. We denote this state by  $\mathcal{A}(x)$ . Metastable states appear at  $x < 1$ ; at values of  $x$  just slightly below 1 they have energies in a small interval  $(E^*, E_m)$  separated from  $E_{\mathcal{A}}$ , the energy of the state  $\mathcal{A}$ , by a gap (cf. figure 6) and exponentially small attraction basins. Thus,  $\mathcal{A}$  is both the optimal state and the state with the largest attraction basin for  $x$  close to 1. In the limit  $x \rightarrow 0$ ,  $\mathcal{A}$  loses both of these special features, namely it is no longer the ground state and also has an exponentially small attraction basin. Generically there are three possible ways in which this can happen, shown schematically in figure 6. Here we sketch the reduced attraction volume,  $\mathcal{P} = W_B/W_{PH}$ , as a function of  $x$ ; for  $x < x_c$ ,  $\mathcal{P}$  becomes exponentially small. We also show schematically the relative energy,  $E_{\mathcal{A}} - E^*$ , between that of state  $\mathcal{A}(x)$  and the lower edge of the ‘continuous’ spectrum. In scenario 1 (see figure 6),  $\mathcal{A}$  retains its optimal status in the vicinity of  $x_c$  even though it loses its large attraction volume. By contrast in case 3 (cf. figure 6),  $\mathcal{A}$  loses first its optimal character and then its large basin. Finally in scenario 2 (cf. figure 6) both special features are lost simultaneously; our complementary numerical studies of the mixed  $p = 2$  and  $p = 3$  disordered spherical models suggest that they are in this class. Solutions of optimization problems that fall into category 1 (and perhaps category

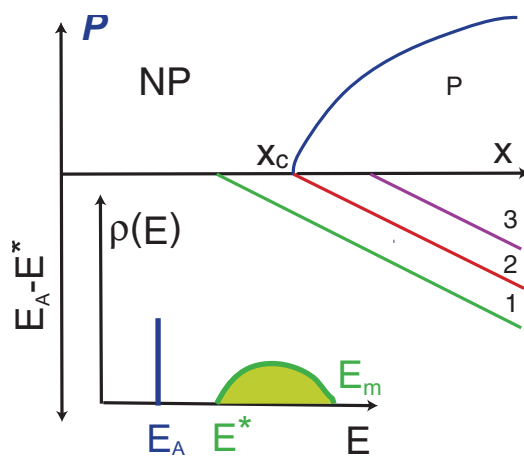


**Figure 6.** A schematic diagram of the reduced typical attraction volume,  $\mathcal{P} = W_B/W_{PH}$ , and the relative energy,  $E_{\mathcal{A}} - E^*$ , as a function of  $x$ ; the three scenarios for  $E_{\mathcal{A}} - E^*$  in the approach to  $x_c$  are described in the text.

2) may be accelerated by noting that the ground state for  $x < x_c$  is continuously connected to  $\mathcal{A}_{x > x_c}$  by tuning the parameter  $x$ . In principle one would start by locating  $\mathcal{A}(x)$  for  $x > x_c$ , a relatively easy problem due to its large attraction volume, and then reduce  $x$  continuously to its value of interest ( $x < x_c$ ). This procedure is reminiscent of simulated annealing where temperature plays a role analogous to that of the tuning parameter  $x$ . It may therefore provide an alternative optimization algorithm for a certain class of  $NP$ -problems.

### Acknowledgments

We thank A Barrat, A Cavagna, S Franz, I Giardina, M Mezard, R Zecchina and particularly A Lopatin for useful discussions.

### Appendix A

Here we sketch the derivation of the thermodynamic properties of the mixed  $p = 2$  and  $p = 3$  spherical spin models in the replica approach. Our main goal is to show that the low-temperature state is described by the one-step replica-symmetry-breaking solution at *all*  $x$  such that  $0 \leq x < 1$ . We follow the standard replica approach developed for  $p$ -spin spherical models [9] with slight modifications implied by the mixed case that we consider here. We introduce order parameter

$$Q_{\alpha\beta} = \frac{1}{N} \sum_i \langle S_{i,\alpha} S_{i,\beta} \rangle$$

and integrate out the spin degrees of freedom. We get the free energy as a function of  $Q_{\alpha\beta}$ :

$$F(Q_{\alpha\beta}) = -\frac{1}{4T} \left\{ \frac{1-x}{3} \sum Q_{\alpha\beta}^3 + \frac{x}{2} \sum Q_{\alpha\beta}^2 \right\} - \frac{T}{2} \text{Tr} \ln Q \quad (\text{A.1})$$

which should be minimized over all  $Q_{\alpha\beta}$  that satisfy the constraint  $Q_{\alpha\alpha} = 1$ . Varying this free energy with respect to  $Q_{\alpha\beta}$  we get an expression for the order parameter:

$$\frac{1}{4T} \left\{ (1-x) Q_{\alpha\beta}^2 + x Q_{\alpha\beta} \right\} + \frac{T}{2} \widehat{Q}_{\alpha\beta}^{-1} = 0 \quad (\text{A.2})$$

where  $\widehat{Q}^{-1}$  denotes matrix inversion.

In order to solve equation (A.2), we multiply it by the  $Q$ -matrix, look for the solution in the form  $\widehat{Q} = \widehat{1} + \widehat{q}$ , and use the Parisi *ansatz* for the matrix  $\widehat{q}$ . Next we exploit the structure of the matrices involved in order to solve the resulting equations in the limit  $n \rightarrow 0$ . More specifically we note that two matrices,  $A$  and  $B$ , that have the block structure of the Parisi *ansatz* and are described by the functions  $A(z)$  and  $B(z)$  in the limit  $n \rightarrow 0$  obey the ‘multiplication rule’

$$(\widehat{A} \widehat{B})_z = - \left[ \int_0^z A_y B_y dy + A_z \int_z^1 B_y dy + B_z \int_z^1 A_y dy + x A_z B_z \right]. \quad (\text{A.3})$$

Using this rule for the matrices  $A_{\alpha\beta} = (1-x)q_{\alpha\beta}^2 + xq_{\alpha\beta}$  (i.e.  $A_z = (1-x)q_z^2 + xq_z$ ) and  $B_{\alpha\beta} = q_{\alpha\beta}$ , we see that for all  $z \neq 1$ , i.e. for all non-diagonal elements of the corresponding matrix, equation (A.3) becomes

$$-(\widehat{A} \widehat{B})_z = (1-x)q_z^2 + (1+x)q_z.$$

Differentiating this equation once with respect to  $z$ , we obtain

$$A'_z \int_z^1 B_y dy + B'_z \int_z^1 A_y dy + z(A'_z B_z + A_z B'_z) = [2(1-x)q_z + (1+x)] q'_z. \quad (\text{A.4})$$

All terms in the preceding equation are proportional to  $q'$ . Assuming that  $q' \neq 0$  (i.e. that the solution is smooth), we divide it by  $q'$  and differentiate it twice with respect to  $z$ . We obtain the equation

$$\frac{q'}{4(1-x)q + 2x} = -\frac{1}{6z(1-x)} \tag{A.5}$$

that clearly does not allow a solution with positive  $q$  and  $q'$ . Thus, we have proved that smooth solutions with  $q' \neq 0$  corresponding to continuous replica-symmetry breaking are *impossible*. Assuming now a one-step replica-symmetry breaking corresponding to a step-like function  $q_z$  at  $z = z_0$ , we get the free energy

$$F(q) = +\frac{1}{4T} \left\{ \frac{1-x}{3} q^3 + \frac{x}{2} q^2 \right\} + \frac{T}{2z_0} \ln \frac{1-q}{1-(1-z_0)q} - \frac{T}{2} \ln(1-q). \tag{A.6}$$

Numerical inspection of this function indicates that at low temperatures it always has a maximum for some  $0 < z_0 < 1$  and  $0 < q < 1$  corresponding to a non-trivial one-step replica-symmetry-breaking solution.

### Appendix B

We now present a skeletal derivation of the number of stable solutions,  $\mathcal{N}(x, e)$ , associated with the system of equations

$$\lambda s_i = 2 \sum_j J_{ij} s_j + 3 \sum_{jk} J_{ijk} s_j s_k \tag{B.1}$$

$$Ne = \sum_{ij} J_{ij} s_i s_j + \sum_{ijk} J_{ijk} s_i s_j s_k. \tag{B.2}$$

and the sum on the spin variables  $\sum_{i=1}^N s_i^2 = N$ . Here  $e$  is the physical energy per spin of the metastable states, and can be conveniently represented as a sum

$$e = \frac{1}{3}(\lambda + \epsilon) \tag{B.3}$$

where  $Ne \equiv \sum_{ij} J_{ij} s_i s_j$  is the energy contribution from the two-spin model.

In order to compute the number of metastable solutions [31], we use the expression

$$\mathcal{N}(\lambda, \epsilon, x) = \int \prod_i ds_i \delta\left(\sum_i s_i^2 - N\right) \delta\left(\frac{\partial H(\lambda)}{\partial s_i}\right) \det\left(\frac{\partial H(\lambda)}{\partial s_i \partial s_j}\right) \delta\left(N\epsilon - \sum_{ij} J_{ij} s_i s_j\right) \tag{B.4}$$

where we perform the calculation at  $T = 0$ , exploiting the absence of subdivision of states for  $T < T_c$ . The determinant in (B.4) can be calculated by noting that

$$A_{ij} \equiv \frac{\partial H(\lambda)}{\partial s_i \partial s_j}$$

is a random symmetric matrix with a semicircular density of eigenvalues distributed in the interval between  $\lambda - \mu_0$  and  $\lambda + \mu_0$ . We will see later that  $\mathcal{N}(\lambda, \epsilon)$  is dominated by  $\lambda = \mu_0$ ; in this case

$$\mathcal{D} = \ln(\det A_{ij}) = \frac{N}{2} \left( 1 + \ln \frac{(2-x)}{2} \right) \tag{B.5}$$

where the  $x$ -dependence of the preceding expression arises from disorder averages over the couplings,  $\langle J_{ij}^2 \rangle$  and  $\langle J_{ijk}^2 \rangle$ . Implementing an integral representation of the  $\delta$ -function, we write

$$\mathcal{N}(\lambda, \epsilon, x) = \int \prod_i ds_i \prod_i \frac{d\phi_i}{2\pi} \frac{d\mu_i}{2\pi} e^{i\mathcal{L} + \mathcal{D}} \delta\left(\sum_i s_i^2 - N\right) \tag{B.6}$$

where the effective Lagrangian is

$$\mathcal{L} = N\mu\epsilon + \lambda \sum_i \phi_i s_i - \mu \sum_{ij} s_i J_{ij} s_j - 2 \sum_{ij} J_{ij} s_j \phi_i - 3 \sum_{ijk} J_{ijk} s_j s_k \phi_i. \quad (\text{B.7})$$

We average the couplings over disorder to obtain

$$\mathcal{L} = N\mu\epsilon + \lambda \sum_i \phi_i s_i + \frac{Ni}{4} \left\{ \frac{\mu^2 x}{2} + \frac{1}{N} \sum_i \phi_i^2 + \frac{(2-x)}{N^2} \left( \sum_i \phi_i s_i \right)^2 + \frac{2\mu x}{N} \sum_i \phi_i s_i \right\}. \quad (\text{B.8})$$

We note that the change of variables  $\vec{\phi} \rightarrow (\phi_{\parallel}, \phi_{\perp})$  where  $\phi_{\parallel} = \phi_i s_i / \sqrt{N}$  has been made, so the effective Lagrangian is no longer a function of  $s_i$ . We can perform the integral over the spin variables in (B.6) with the result

$$\mathcal{N}(\lambda, \epsilon, x) = \int \frac{d\mu}{2\pi} \frac{d\phi_{\parallel}}{2\pi} \prod_{v=1}^{N-1} \frac{d\phi_{\perp}^v}{2\pi} e^{i\tilde{\mathcal{L}} + \tilde{\mathcal{D}}} \quad (\text{B.9})$$

where

$$\tilde{\mathcal{L}} = N\mu\epsilon + \frac{iNx\mu^2}{8} + \lambda\sqrt{N}\phi_{\parallel} + \frac{1}{4} \left\{ (\phi_{\parallel}^2 + \phi_{\perp}^2) + (2-x)\phi_{\parallel}^2 + 2\mu x\sqrt{N}\phi_{\parallel} \right\} \quad (\text{B.10})$$

and

$$\tilde{\mathcal{D}} = \frac{N}{2} \{2 + \ln \pi(2-x)\}. \quad (\text{B.11})$$

Integrating over the remaining variables  $\mu$ ,  $\phi_{\parallel}$ , and  $\phi_{\perp}$  in (B.9) and using the relation  $\epsilon = 3e - \lambda$ , we obtain

$$\ln \mathcal{N}(\lambda, e, x) = \frac{N}{2} \left\{ 2 + \ln(2-x) - \frac{2\lambda^2}{3-x} - \frac{12(e(x-3) + \lambda)^2}{(3-x)x(1-x)} \right\}. \quad (\text{B.12})$$

In order to determine the total number of metastable states, we maximize  $\mathcal{N}(\lambda, x, e)$  with respect to  $\lambda$  subject to the constraint that  $\lambda > \mu_0$  where

$$\mu_0 = 2\sqrt{N\langle A_{ij}^2 \rangle} = \sqrt{2(2-x)} \quad (\text{B.13})$$

to ensure that all eigenvalues of  $A_{ij}$  are positive, so that we are only counting stable states. We have checked that for  $0 < x < 1$  the main contribution to  $\mathcal{N}(\lambda, x, e)$  comes from  $\lambda = \mu_0$ . This implies that at any energy for  $0 < x < 1$  the majority of the states are marginally stable. In order to obtain the total number of states, we maximize  $\mathcal{N}(x, e, \lambda = \mu_0)$  with respect to energy which yields the result (20).

## References

- [1] For a review of these problems from the perspective of spin glasses see Mezard M, Parisi G and Virasoro M A 1987 *Spin Glass Theory and Beyond* (Singapore: World Scientific)
- [2] Wolynes P G 1997 *Annu. Rev. Phys. Chem.* **48** 545
- [3] Finkelstein A V and Badretolinov A Y 1997 *Mol. Biol.* **31** 391
- [4] Dill K A and Chan H S 1997 *Nat. Struct. Biol.* **4** 10
- [5] Dobson C M, Sali A and Karplus M 1998 *Angew. Chem. Int. Edn* **37** 868
- [6] Kirkpatrick S, Gelatt C D and Vecchi M P 1987 *Science* **220** 339
- [7] For a discussion of a specific coding problem of this type see Bouchaud J P and Mezard M 1994 *J. Physique I* **4** 1109
- [8] Optimization using quantum tunnelling processes is an alternative proposal for such problems. Quantum annealing has been explored numerically by Kadowaki T and Nishimori H 1998 *Preprint cond-mat/9804280*

- and it has recently been studied experimentally in a disordered magnet by Brooke J, Bitko D, Rosenbaum T F and Aeppli G 1999 *Science* **284** 779
- [9] Crisanti A and Sommers H-J 1992 *Z. Phys. B* **87** 341
- [10] Kosterlitz J M, Thouless D J and Jones R C 1976 *Phys. Rev. Lett.* **36** 1217
- [11] Crisanti A and Sommers H-J 1995 *J. Physique I* **5** 805
- [12] Cavagna A, Giardina I and Parisi G 1998 *Phys. Rev. B* **57** 11 251
- [13] Barrat A and Franz S 1998 *J. Phys. A: Math. Gen.* **31** L119
- [14] Gross D J and Mezard M 1984 *Nucl. Phys. B* **240** 431
- [15] For a review of the out-of-equilibrium properties of these models see  
Bouchaud J-P, Cugliandolo L F, Kurchan J and Mezard M 1998 *Spin Glasses and Random Fields* ed A P Young (Singapore: World Scientific) pp 161–225
- [16] Kurchan J, Parisi G and Virasoro M A 1993 *J. Physique I* **3** 1819
- [17] Cavagna A, Giardina I and Parisi G 1997 *J. Phys. A: Math. Gen.* **30** 7021
- [18] Crisanti A, Horner H and Sommers H-J 1993 *Z. Phys. B* **92** 257
- [19] Cugliandolo L F and Kurchan J 1993 *Phys. Rev. Lett.* **71** 173  
Cugliandolo L F and Kurchan J 1994 *J. Phys. A: Math. Gen.* **27** 5749
- [20] Bouchaud J P, Cugliandolo L, Kurchan J and Mezard M 1996 *Physica A* **226** 243
- [21] The mapping between periodic and disordered systems was first suggested by  
Kirkpatrick T R and Thirumalai D 1987 *Phys. Rev. Lett.* **58** 2091  
Kirkpatrick T R and Thirumalai D 1987 *Phys. Rev. B* **36** 5388  
Kirkpatrick T R, Thirumalai D and Wolynes P G 1989 *Phys. Rev. B* **40** 104
- [22] Parisi G 1995 *Twenty Five Years of Non-Equilibrium Statistical Mechanics; Proc. 13th Sitges Conf.* ed J J Brey, J Marro, J M Rubi and M San Miguel (Berlin: Springer) pp 135–42
- [23] Franz S and Herz J 1995 *Phys. Rev. Lett.* **74** 2115
- [24] Chandra P, Ioffe L B and Sherrington D 1995 *Phys. Rev. Lett.* **75** 713  
Chandra P, Feigelman M V and Ioffe L B 1996 *Phys. Rev. Lett.* **76** 4805  
Chandra P, Feigelman M V, Ioffe L B and Kagan D M 1997 *Phys. Rev. B* **56** 11 553
- [25] Gotze W 1984 *Z. Phys. B* **56** 139  
Leutheusser E 1984 *Phys. Rev. A* **29** 2765
- [26] Houghton A, Jain S and Young P 1983 *Phys. Rev. B* **28** 290
- [27] Franz S and Parisi G 1995 *J. Physique* **5** 1401
- [28] Barrat A, Burioni R and Mezard M 1996 *J. Phys. A: Math. Gen.* **29** L81
- [29] Lopatin A and Ioffe L B 1999 *Preprint cond-mat/9907135*  
Lopatin A and Ioffe L B 2000 *Phys. Rev. Lett.* **84** 4208
- [30] Monasson R, Zecchina R, Kirkpatrick S, Selman B and Troyansky L 1999 *Nature* **400** 133
- [31] Tanaka F and Edwards S F 1980 *J. Phys. F: Met. Phys.* **10** 1769  
Bray A J and Moore M A 1980 *J. Phys. C: Solid State Phys.* **13** L469  
De Dominicis C *et al* 1980 *J. Physique* **41** 923